Skvarla, J.; Uchman, M.; Prochazka, K.; Tosner, Z.; Haramus, V.M.; Pispas, S.; Stepanek, M.:

Micellization of Zonyl FSN-100 fluorosurfactant in aqueous solutions

In: Colloids and Surfaces A (2013) Elsevier

DOI: 10.1016/j.colsurfa.2013.11.021

Micellization of Zonyl FSN-100 Fluorosurfactant in Aqueous Solutions

Juraj Škvarla[a], Mariusz Uchman[a], Karel Procházka[a], Zdeněk Tošner[b], Vasyl Garamus[c], Stergios Pispas[d] and Miroslav Štěpánek[a,*]

[a]*Department of Physical and Macromolecular Chemistry and* [b]*NMR Laboratory, Faculty of Science, Charles University in Prague, Hlavova 2030, 128 40 Prague 2, Czech Republic. Fax: +420 2 2491 9752; Tel: +420 2 2195 1290; E-mail: stepanek@natur.cuni.cz*

[c]*Helmholtz-Zentrum Geesthacht, Centre for Materials and Coastal Research, D-21502 Geesthacht, Germany*

[d]*Theoretical & Physical Chemistry Institute, National Hellenic Research Foundation, 48 Vassileos Constantinou Avenue, 11635 Athens, Greece*

Abstract. We report on micellization of nonionic fluorosurfactant Zonyl FSN-100 in aqueous solutions studied by means of NMR, light and small-angle X-ray scattering, surface tension measurements, isothermal titration calorimetry and fluorescence spectroscopy. The results allow for determination of basic parameters of Zonyl FSN-100 association like critical micellar concentration, size and association number of Zonyl FSN-100 micelles which have a core-shell structure with the core of fluorocarbon chains and the shell of oligo(ethylene oxide) chains. Time-resolved fluorescence spectroscopy studies using 1,6-diphenyl-1,3,5-hexatriene (DPH) as a fluorescent probe indicate that DPH can be solubilized in the micelles despite the general assumption about the immiscibility of hydrocarbon compounds with the fluorocarbon core of the micelles.

Introduction

Fluorinated amphiphilic compounds[1] have received great attention in the past several decades due to their properties which differ in many respects from their counterparts with hydrocarbon aliphatic chains and which are interesting for potential applications in medicine (oxygen delivery[2]) and technology (emulsifiers,[3] hydrophobic surface layers[4]). Since the fluorocarbon chain is stiffer and bulkier than the hydrocarbon chain of the same length,

interfaces formed by fluorinated surfactants (FS) tend to be less curved than those of single-chain hydrocarbon surfactants, so that FS self-assemble in vesicles or wormlike micelles rather than in spherical micelles.[5-7] Low polarizibility of fluorine results in weaker dispersion forces between fluorocarbon tails as compared with hydrocarbons, which causes fluorocarbon chains being both hydrophobic and lipophobic. Co-assembly of FS with hydrocarbon amphiphiles often leads to multicompartment structures in which fluorinated chains form segregated domains.[8]

Zonyl FSN-100, $F(CF_2CF_2)_{1-9}CH_2CH_2O(CH_2CH_2O)_{0-25}H$[9] is a representative of a nonionic fluorinated surfactant, which was produced by DuPont until 2010. Despite the fact that it was the subject of a number of studies dealing with its applications as an emulsification of plasmid DNA delivery systems,[9] stabilization of gold nanoparticles[10] or formation of superhydrophobic self-assembled monolayers on gold,[4] no study of its self-assembly in solution has been published so far.

In this article, we study association of Zonyl FSN-100 in aqueous solutions. We focus (i) on the process of formation of FSN-100 micelles in water, which is followed by isothermal titration calorimetry and surface tension measurements and (ii) on the structure of FSN-100 micelles in water, which is characterized by means of light and small-angle X-ray scattering.

Experimental

Materials. Zonyl FSN-100 fluorosurfactant, 1,6-difenyl-1,3,5-hexatriene (DPH) and dioxane were purchased from Sigma-Aldrich. Deionized water was used for preparation of FSN-100 aqueous solutions. For fluorescence anisotropy measurements, 2 mL of 5 mM stock solution of DPH in dioxane were added to 2 mL of 10 g L^{-1} Zonyl FSN-100 solution.

Methods. *NMR Measurements*. ^{1}H, ^{13}C and ^{19}F NMR measurements were carried out at 25°C in D_2O (Fluka, 99.5 % D) using a Bruker Avance III 600 MHz and Varian Inova 400 MHz instruments. For quantitative experiments (recycle delay 30 s), 2,2,2-trifluoroethanol (TFE) was used as an internal standard.

*Surface Tension Measurements***.** Surface tension of FSN-100 solutions was measured at 25°C by the Wilhelmy plate method using a Krüss K100 tensiometer.

Isothermal Titration Calorimetry (ITC). ITC measurements were performed at 25 ºC with a Nano ITC isothermal titration calorimeter (TA Instruments – Waters LLC, New Castle, DE).

The microcalorimeter consisted of a reference cell and a sample cell both of 183 μL volume (24 karat gold). The sample cell was connected to a 50 μL syringe, the needle of which was equipped with a flattened, twisted paddle at the tip, which ensured continuous mixing of the solutions in the cell rotating at 250 rpm. Titration measurements were carried out by consecutive 2.06 μL injections of an aqueous 2.1 mM Zonyl FSN-100 in aqueous solution from the syringe into the sample cell filled with water. A total of 24 consecutive injections were performed. The delay between two consecutive injections was 250 s. These injections replace a part of the solution in the sample volume, and the changed concentration is considered in the calculation of the sample concentration. By this method, the differential heat of mixing is determined for discrete changes of composition. The data were analyzed using the NanoAnalyze software.

Light Scattering (LS). The light scattering setup (ALV, Langen, Germany) consisted of a 22 mW He-Ne laser, operating at the wavelength λ = 632.8 nm, an ALV CGS/8F goniometer, an ALV High QE APD detector and an ALV 5000/EPP multibit, multitau autocorrelator. Both static and dynamic LS measurements were carried out at 25°C in the angular range 30° to 150° corresponding in aqueous solutions to the scattering vector magnitudes q ranging from 6.8 μm^{-1} to 25.6 μm^{-1}.

Refractive index increment measurements were carried out at 25°C using a Wyatt T-ReX differential refractometer. The aqueous solutions of FSN-100 in four different concentrations were pumped into the refractometer by a syringe driven by a 78-9100C Cole Parmer syringe drive with a flow rate of 1mL/min. The refractive index value was determined from the slope of the plot of the refractive index versus concentration.

Dynamic light scattering (DLS) measurements were evaluated by fitting the measured electrid field, $g^{(1)}(\tau,q)$, calculated from the measured time autocorrelation functions of the scattered light intensity, $g^{(2)}(\tau,q)$, as $g^{(1)}(\tau,q) = [g^{(2)}(\tau,q) - 1]^{1/2}$.

Small-angle X-Ray Scattering (SAXS). SAXS experiments were performed on the P12 BioSAXS beamline at the storage ring PETRA III of the Deutsche Elektronen Synchrotron (DESY, Hamburg, Germany) at 20 °C using a Pilatus 2M detector and synchrotron radiation with the wavelength of λ = 0.1 nm. The sample-detector distance was 3 m, allowing for measurements in the q-range interval from 0.11 to 4.4 nm^{-1}. The q range was calibrated using the diffraction patterns of silver behenate. The experimental data were normalized to the incident beam intensity, corrected for non-homogeneous detector response, and the background scattering

of the solvent was subtracted. The solvent scattering was measured before and after the sample scattering to control for possible sample holder contamination. Eight consecutive frames comprising the measurement of the solvent, sample, and solvent were performed. No measurable radiation damage was detected by a comparison of eight successive time frames with 15 s exposures. The final scattering curve was obtained using the program PRIMUS by averaging the scattering data collected from the different frames and analyzed by means of the SASfit 0.93.2 software.[11]

Fluorescence spectroscopy. Fluorescence measurements were performed using a FluoroLog 3-22 spectrometer (Horiba – Jobin Yvon, France) equipped with a FluoroHub time-correlated single photon counting module and Glan-Thompson polarizers. The excitation source was a pulsed diode laser (NanoLED) with the emission maximum at 378 nm and the pulse fwhm about 200 ps, operated at the repetition frequency of 1 MHz. Obtained fluorescence decays were fitted by a double-exponential decay model using the Marquardt-Levenberg nonlinear least-squares method.

Results and Discussion

Determination of molar mass and chain lengths of FSN-100 by NMR. Since the lengths of both hydrophilic and hydrophobic chains of FSN-100 are variable, we measured quantitative ^{1}H, ^{13}C, and ^{19}F NMR spectra of 20 mg/mL FSN-100 solution in D_2O with TFE as an internal standard in order to determine the fluorine and hydrogen content in the used FSN-100 sample; all the spectra are shown in the Supporting Information. The integral over the isolated signal of CH_2CF_2 protons was used to calculate the molar concentration of FSN-100 with respect to the known concentration of TFE. The measurements and calculations yield the molecular formula of the used FSN-100 sample, $CF_3(CF_2)_{\langle 7.4 \rangle}(CH_2CH_2O)_{\langle 13.7 \rangle}H$ corresponding to the average molar mass of 1044 g mol^{-1}.

When studying solution self-assembly behavior of FSN-100, it is, however, necessary to keep in mind that these values are averages and that the heterogeneity of both fluorocarbon and oligo(ethylene oxide) chains can lead not only to polydisperse micelles and less distinct unimer-to-micelles transitions but even to formation of self-assembled nanoparticles with various morphologies which will coexist in the solution at the same surfactant concentration.

Measurements of critical micelle concentration. In order to determine the critical micelle concentration of FSN-100, we employed surface tension, isothermal titration calorimetry and ^{19}F NMR measurements. Fig. 1 shows the surface tension of FSN-100 aqueous solution, γ, as a function of the logarithm of the surfactant concentration up to C = 5 mg/mL. The curve contains two breaks at 0.010 and 0.047 mmol L^{-1}. A similar behavior was observed for Pluronic copolymers in aqueous solutions,[12] where the presence of the low-concentration break was ascribed to the conformational transition of the polymer chain. In the case of FSN-100, the length of the hydrophilic chain is sufficient to exhibit a similar transition.

The slope of the γ vs. ln C curve is proportional to the excess absorbed amount of the surfactant at air-water interface *per* unit area, $\Gamma = -(\partial\gamma/\partial \ln C)_{T,p}/RT$, where R is the gas constant and T temperature. Below the low-concentration break, the fit provides the value $\Gamma = 3.91\times10^{-10}$ mol cm^{-2}, corresponding to the surface area of 0.42 nm^2. The high concentration break at 0.047 mmol L^{-1} indicates the cmc of the surfactant. Both parameters can be compared with those for the similar fluorosurfactant[13] $CF_3(CF_2)_5CH_2O(CH_2CH_2O)_3CH_3$ with $\Gamma = 4.37\times10^{-10}$ mol cm^{-2} and cmc = 0.08 mmol L^{-1}.

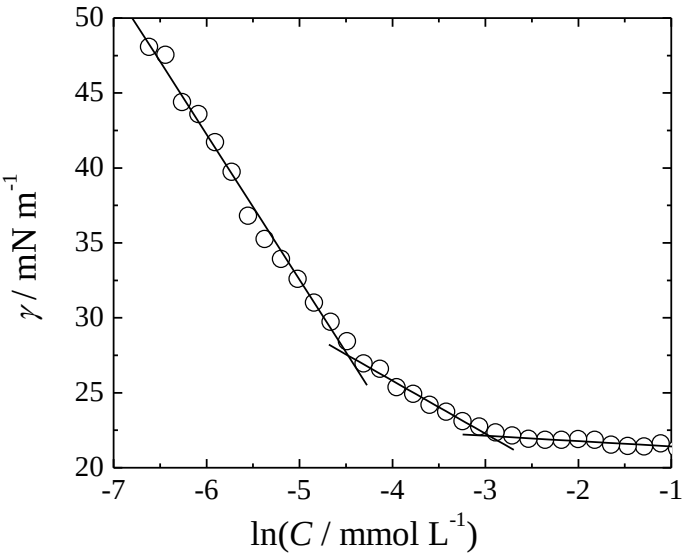

Fig. 1. Surface tension of FSN-100 aqueous solution, as a function of FSN-100 concentration.

The evaluation of ITC data (Fig. 2) is difficult because the demicellization contribution to the observed enthalpy changes decreases gradually with the FSN-100 concentration. While the inflection point indicating the cmc can be found, the plateau values are not accessible and the micellization enthalpy cannot thus be determined. This behavior can again be explained by the heterogeneity of FSN-100 which leads to complex multiple micellization equilibria, especially near the cmc region before the excess of uniform micelles is formed. The observed cmc value, 8.8×10^{-2} mmol L^{-1}, is roughly comparable with that from the tensiometric measurement.

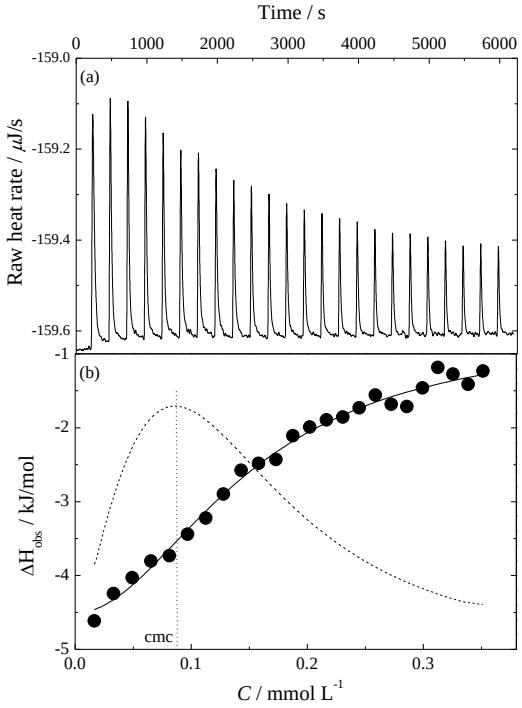

Fig. 2. (a) Heat flow rate during the injections of 2.06 mL portions of 2.1 mM FSN-100 solution into water. (b) Observed enthalpy change as a function of FSN-100 concentration (circles) and the fit by the sigmoidal function. The dashed curve is the first derivative of the fitted function.

^{19}F NMR. As the third technique for the determination of cmc, we used the method based on the fact that chemical shifts of NMR signals of the surfactant molecules in solution may differ significantly from those embedded in micelles. Due to the fast dynamic exchange of unimers among the micelles, the resulting chemical shift of such a signal in a micellar system is the number average of the values for the micelle-bound surfactant and the free surfactant. Fig. 3a shows the concentration changes of the ^{19}F NMR spectrum of FSN-100 in D_2O in the region from –116 to –112 ppm. One of the environment-sensitive CF_2 signals appears at –113.1 ppm for

the free FSN-100 in 0.05 mmol L^{-1} solution and at –114.2 ppm for FSN-100 in micelles in 5 mmol L^{-1}. Above 0.1 mmol L^{-1}, the signal moves upfield gradually with the increasing concentration as the micelles are formed (the concentration dependence is shown in Fig. 3b). Hence, the NMR measurement supports the results of surface tension and ITC measurements showing that the cmc of the system is close to 0.1 mmol L^{-1}.

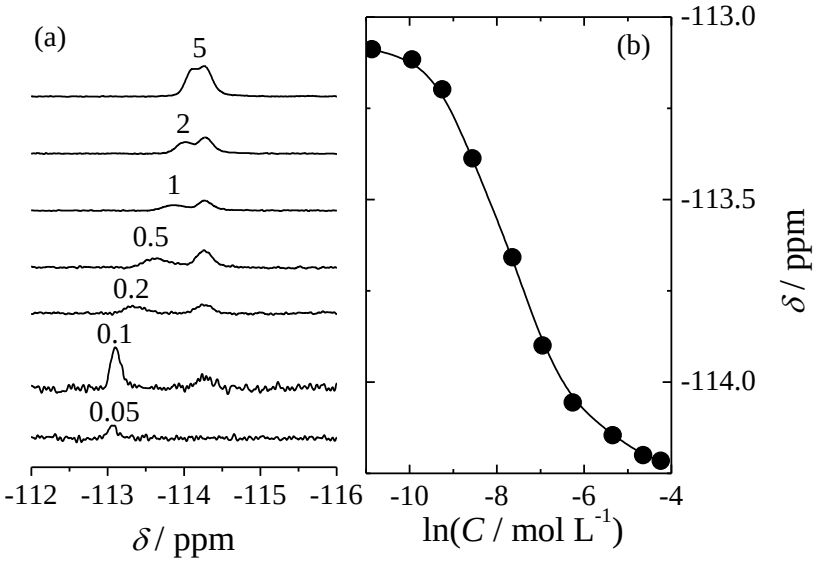

Fig. 3. (a) ^{19}F NMR spectra of FSN-100 aqueous solution (region from –112 to –116 ppm) in D_2O at various concentrations (indicated above the curves, in mmol L^{-1}). (b) Concentration dependence of an environment-sensitive chemical shift of the signal shown in Fig. 3a.

The second part of the study was aimed at the characterization of FSN-100 micelles in water at the room temperature. While it can be expected that FSN-100 self-assembly in aqueous solution has segregated fluorocarbon and oligo(ethylene oxide) chains, the shape of the particles is difficult to predict because of the polydispersity of the surfactant: The self-assembly of the stiff and bulky fluorocarbon chains requires a less curved interface (like in bilayered vesicles or cylindrical micelles), while the attached flexible hydrophilic chains with the relatively greater length favors spherical morphology. In order to elucidate the structure of FSN-100 self-assembly in water, we carried out LS and SAXS measurements.

Light scattering. Light scattering is less sensitive for studies of FS aqueous solution than for aqueous solutions of hydrocarbon surfactants because of low refractive index increments of FS in water (the refractive index increment of FSN-100 in water is only 0.080 mL/g) which

results in low excess scattering intensities of FS aqueous solutions. In the case of FSN-100, reliable light scattering measurements in water can be done for concentrations greater than ~1 mg/mL (~0.7 mmol L^{-1}, that is, above its cmc), however, LS can still be used for determination of the hydrodynamic radius and molar mass of FSN-100 micelles.

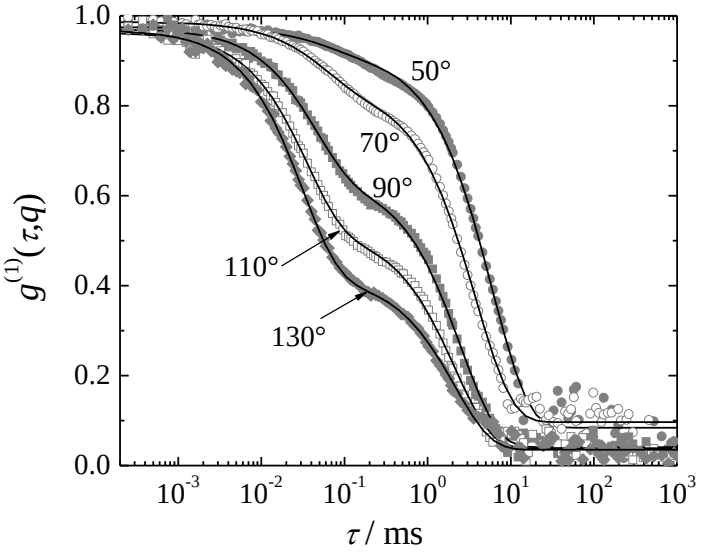

Fig. 4. Electric field autocorrelation functions for DLS of 20 g/L FSN-100 aqueous solution at various scattering angles.

Electric field autocorrelation functions, $g^{(1)}(\tau, q)$, of 20 g/L FSN-100 aqueous solution at various scattering angles are shown in Fig. 4. The $g^{(1)}(\tau, q)$ functions are distinctly double-exponential, with the relaxation times proportional to q^{-2} indicating that both times correspond to fluctuations caused by diffusive motion of the scatterers. Fig. 5 shows the angular dependences of the apparent diffusion coefficients D_1 and D_2 and of the relative amplitude f for the scattering of the particles with the diffusion coefficient D_1, obtained from fit of the $g^{(1)}(\tau, q)$ functions by by the equation

$$g^{(1)}(\tau, q) = A\left[f\,\mathrm{e}^{-D_1 q^2 \tau} + (1-f)\mathrm{e}^{-D_2 q^2 \tau}\right] + B \qquad (1)$$

where A is the amplitude and B is the baseline constant. The average values of the diffusion coefficients in the angular range from 70° to 130° are $D_1 = 6.5\times10^{-11}$ m^2 s^{-1} and $D_2 = 1.04\times10^{-12}$ m^2 s^{-1} which corresponds to hydrodynamic radii $R_{H,1} = 3.1$ nm and $R_{H,2} = 194$ nm. Since the form factor for the large particles decreases strongly with increasing q, while the scattering from the small particles is independent on the scattering angle, the relative amplitude f increases with the increasing q.

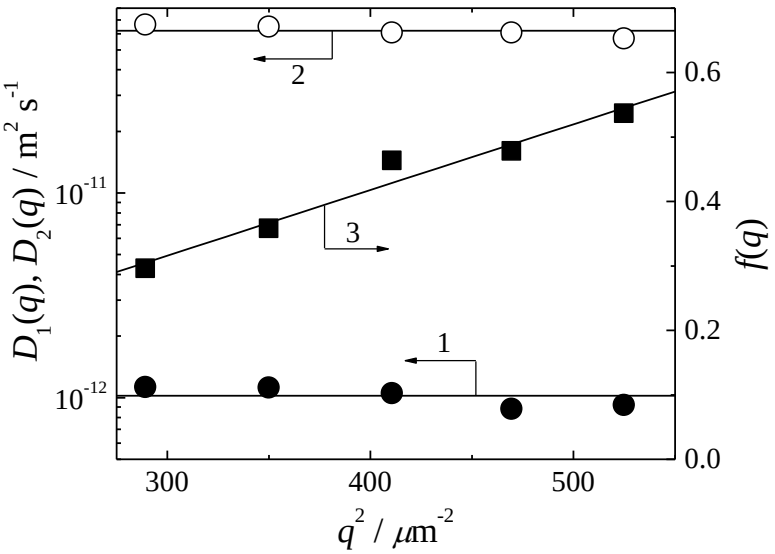

Fig. 5. Apparent diffusion coefficients D_1, D_2 (curves 1 and 2, respectively) and the relative amplitude of the mode with the diffusion coefficient D_1 (curve 3) as functions of q^2.

The presence of two types of particles with very different sizes can be ascribed to the already mentioned heterogeneity of FSN-100 composition which may lead to the segregation of the surfactant molecules into different self-assemblies according to their hydrophobic and hydrophilic chain lengths. While the radius $R_{H,1}$ can be ascribed to FSN-100 micelles, $R_{H,2}$ probably corresponds to FSN-100 vesicles formed by a fraction of FSN-100 molecules with long hydrophobic and short hydrophilic chains. However, as the difference in particles sizes reaches almost two orders of magnitude, the scattering cross-section of the micelles is negligible as compared with the large particles, which implies that at comparable scattering amplitudes of the two followed fluctuation processes, the amount of the large particles responsible for the slower fluctuation is negligible. For this reason we further focus on small FSN-100 micelles only.

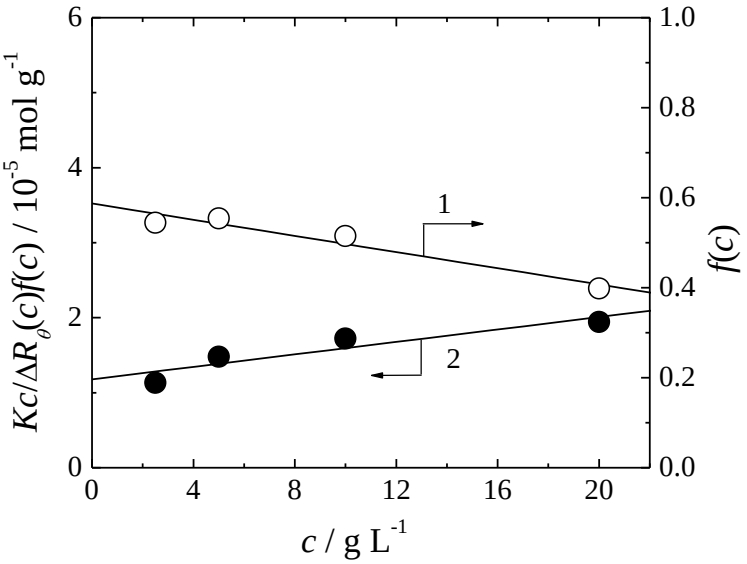

Fig. 6. Zimm plot for the SLS of FSN-100 aqueous solutions at the scattering angle θ = 90° (curve 1) and the relative amplitude of the mode with the diffusion coefficient D_1 (curve 2) as functions of c.

In order to determine the molar mass of FSN-100 micelles, the scattering from the large particles has to be subtracted from the overall scattering from the sample. The contribution of the FSN-100 micelles to the excess Rayleigh ratio, ΔR_θ, of the solution can be expressed by means of the relative amplitude f as $\Delta R_\theta^{\text{mic}} = f\Delta R_\theta$. Taking into account that the mass fraction of FSN-100 in large particles is negligible, and that the form factor of the micelles in the q range of the light scattering measurement is $P_{\text{mic}}(q) \approx 1$, the weight average molar mass, M_{w}, of FSN-100 micelles can be found by fitting the data by the Zimm equation,

$$\frac{Kc}{\Delta R_\theta(c) f(c)} = \frac{1}{M_{\text{w}}} + 2A_2 c \qquad (2)$$

where A_2 is the second osmotic virial coefficient of the solution and $K = 4\pi^2 n_0^2 (\mathrm{d}n/\mathrm{d}c)^2/\lambda^4 N_{\text{A}}$ is the optical constant in which n_0 is the refractive index of the solvent, dn/dc is the refractive index increment of the solution and N_{A} is the Avogadro constant. Fig. 6 shows the values of f and

$Kc/f\Delta R$ as functions of c at the scattering angle of 90°. The fit of the eq. 2 to the data in Fig. 6 yields the value of the molar mass of the micelles, $M_w = 8.5\times10^4$ g mol^{-1}.

Small-Angle X-Ray Scattering. SAXS measurement was used to confirm the assumption that FSN-100 forms spherical micelles composed of the compact core formed by $CF_3(CF_2)_{\langle 5.54\rangle}$ chains and the swollen shell of the hydrated $H(OCH_2CH_2)_{\langle 13.88\rangle}$ chains. The simplest model of the spherical core-shell particle, assuming both the homogenous core and the homogeneous shell, did not lead to satisfactory fits. Therefore the scattering data were fitted by the Pedersen-Gerstenberg (PG) model[14] treating FSN-100 micelles as hard spheres with attached Gaussian chains. Intermicellar interactions were described by the hard sphere structure factor[15] in the monodisperse approximation. (The full expression for the scattering function is provided as Supplementary Information for this article.) The scattering curve measured for 10 mg/mL FSN-100 aqueous solution and the fit of the experimental data by the PG model with the hard sphere structure factor are shown in Fig. 7. The parameters obtained from the fit are: (i) the core radius, R = 1.36 nm, (ii) the gyration radius of a chain in the shell, r = 0.84 nm, (iii) aggregation number, N_{agg} = 102, (iv) the excess scattering lengths of chains forming the core and the shell, $b_c = 9.1\times10^{-12}$ cm and $b_s = 34.5\times10^{-12}$ cm, the hard sphere interaction radius R_{sph} = 4.32 nm and the excluded volume fraction of the micelles in the shell, $\varphi = 2.56\times10^{-2}$.

Although the PG model was developed for block copolymer micelles with much longer chains than in the case of FSN-100, it appeared to be a good approximation of the radial dependence of the scattering length density of in FSN-100 micelles. Parameters obtained from the fit are in a good accordance with other experimental data for the FSN-100 solution, as we show below.

(i) *Gyration radius of the chains in the shell*. The radius of the micelles, R_{mic} = 3.04 nm, calculated as $R_{mic} = R + 2r$, compares very well with the hydrodynamic radius, R_H = 3.1 nm, from DLS.

(ii) *Aggregation number.* Using the aggregation number, N_{agg} = 102, obtained from the fit and the mean molar mass of FSN-100, M_{FSN} = 1044 g mol^{-1}, we can calculate the molar mass of the micelles $M_{mic}^{SAXS} = 10.7\times10^5$ which is roughly comparable with the value found by SLS, $M_{mic} = 8.5\times10^5$.

(iii) *Excluded volume fraction.* Assuming the molar mass of 8.5×10^4 g mol^{-1} (SLS), the mass concentration of the solution, c = 10 mg/mL, and the hard sphere interaction radius R_s =

4.32 nm, the excluded volume fraction, $\varphi^{theor} = 4\pi R_{sph} N_A / 3M_{mic} = 2.39\times10^{-2}$ is similar to the values from the fit, $\varphi = 2.56\times10^{-2}$.

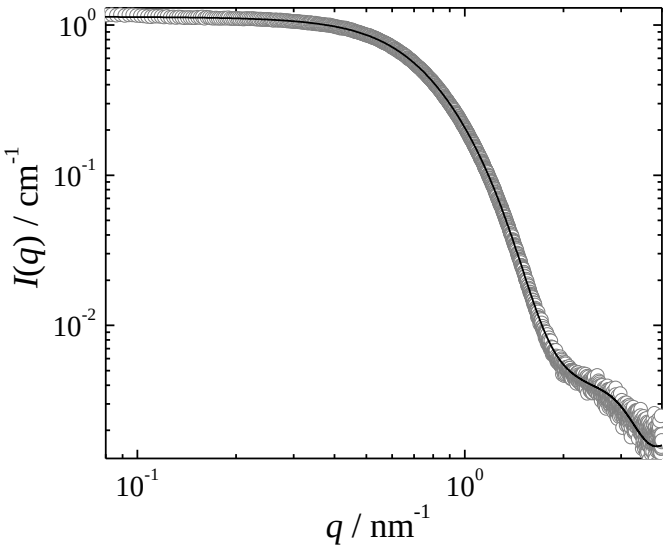

Fig. 7. SAXS curve of 10 mg/mL FSN-100 aqueous solutions. Open circles: experimental data, solid line: fit of the experimental data by the Pedersen-Gerstenberg model.

Fluorescence measurements. In order to study the interaction of FSN-100 micelles with low-molar-mass compounds, we carried out a series of fluorescence measurements using 1,6-diphenyl-1,3,5-hexatriene (DPH) as a hydrophobic fluorescent probe. Since DPH emission is environmentally sensitive due to solvent-induced energy shift effects on the close-lying excited states,[16] DPH can be used as a probe for microenvironment polarity.

Fig. 8. shows fluorescence emission decay of 5 μM DPH in 10 g L^{-1} aqueous solution of FSN-100 and its fit by the triple exponential model

$$I(t) = \sum_{i=1}^{3} \alpha_i \mathrm{e}^{-t/\tau_i} \qquad (3)$$

where α_1= 0.152, α_2 = 0.057, α_3 = 0.091 are the amplitudes and τ_1 = 6.82 ns, τ_2 = 2.52, ns τ_3 = 0.60 ns are the lifetimes. The multiexponential decay behavior suggests that DPH is incorporated into FSN-100 micelles where it experiences different microenvironments due to different

polarities and polarizibilities of the inner core, the interfacial layer and the shell. In order to corroborate this assumption, we performed the time-resolved fluorescence anisotropy measurement. Inset in Fig. 8 shows the anisotropy decay of 5 μM DPH in 10 g L^{-1} aqueous solution of FSN-100 and its fit by the formula,[17]

$$r(t) = (r_0 - r_\infty)\left[\beta \mathrm{e}^{-t/\varphi_1} + (1-\beta)\mathrm{e}^{-t/\varphi_2}\right] + r_\infty \qquad (4)$$

where r_0 = 0.388 and r_∞ = –0.005 are the initial and residual anisotropies, φ_1 = 4.32 ns and φ_2 = 1.10 ns are the rotational correlation times and β = 0.47 is the relative amplitude for the correlation time φ_1. The obtained r_0 value agrees with the earlier reported DPH anisotropy in hydrocarbon glasses at low temperatures,[18] the residual anisotropy is zero within the range of the experimental error. The mean rotational correlation time, $\langle\varphi\rangle = \beta\varphi_1 + (1-\beta)\varphi_2$ = 2.64 ns, can be used for the calculation of the volume of the rotating unit according to the formula $V = \langle\varphi\rangle k_B T/\eta$, where k_B is the Boltzmann constant and η is the solvent viscosity. The resulting value $V = 1.09\times10^{-26}$ m^3 corresponds to the volume of a sphere with the radius 2.95 nm, which compares very well with the hydrodynamic radius of a FSN-100 micelle. This result proves that the DPH molecules are embedded in FSN micelles and their fluorescence depolarization dynamics is controlled by the rotational diffusion of the micelles. The fact that DPH is solubilized by FSN-100 is somehow surprising because hydrocarbon fluorophores such as pyrene were reported not to interact with FS micelles,[19] so that the fluorescence studies of FS have been carried out using fluorophores with fluorocarbon chains.[20]

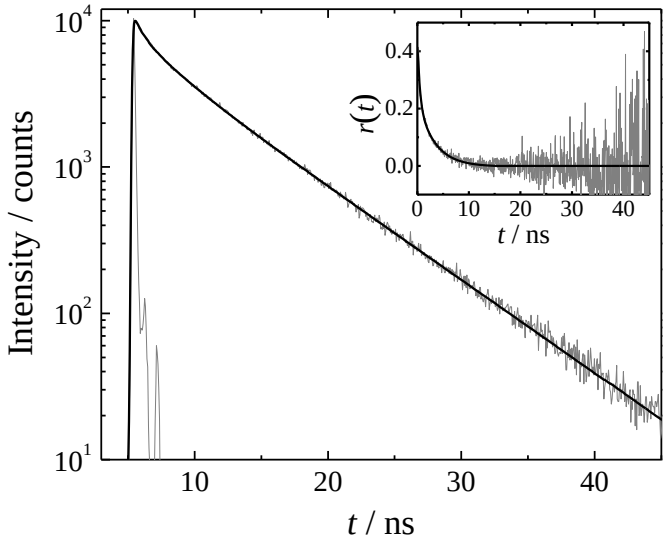

Fig. 8. DPH emission decay (excitation: 378 nm, emission, 425 nm) in 10 mg/mL FSN-100 aquous solution. Inset: DPH anisotropy decay in the same system.

Conclusions

We have studied aqueous solutions of the perfluorinated surfactant Zonyl FSN-100 at 25°C by means of tensiometry, isothermal titration calorimetry, light and small-angle X-ray scattering and by fluorescence spectroscopy. The study brought the following pieces of information about the association behavior of FSN-100 and about the structure of FSN-100 micelles:

1) We have obtained the values of cmc of FSN-100 in aqueous solution by means of tensiometry and ITC. ITC studies have shown that adsorption of FSN-100 at the air-water interface and its micellization in aqueous solution are influenced by the nonuniform composition of the surfactant.

2) We have studied the size and shape of FSN-100 micelles by a combination of static and dynamic LS and SAXS. Light scattering measurements have shown that trace amount of large particles (possibly vesicles) with the hydrodynamic radius about 200 nm coexist with FSN-100 micelles with R_H = 3 nm. The SAXS of the micelles can be described by the Pedersen-Gerstenberg model, which suggests that their structure resembles that of block copolymer

micelles. The fit allowed for determination of the core and shell dimensions. The aggregation number obtained from the PG model is in good accordance with the molar mass of FSN-100 obtained from static light scattering.

3) Time-resolved fluorescence measurements with DPH as a hydrophobic fluorescent probe have shown that DPH can be solubilized in FSN-100 micelles. This result is rather surprising because fluorocarbon domains in micelles formed by FS surfactants are both hydrophobic and lipophobic and it was reported that fluorescent probes do not solubilize in domains of fluorocarbon chains in FS micelles unless they possess a fluorocarbon tail.

Acknowledgments

The authors thanks Dr Edyta Kuliszewska from ICSO, Kędzierzyn-Koźle, Poland, for surface tension measurements. Financial support from the Ministry of Education of the Czech Republic (Long-Term Research Project MSM0021620857, Grant 7AMB13PL026) and Czech Science Foundation (grants P106/12/0143 and P208/12/P236) is gratefully acknowledged.

References

(1) Matsuoka, K.; Moroi, Y. Micellization of fluorinated amphiphiles. *Current Opinion Colloid Interface Sci.* **2003**, *8*, 227–235.

(2) Riess, J.G. Blood substitutes and other potential biomedical applications of fluorinated colloids. *J. Fluorine Chem.* **2002**, *114*, 119 –26.

(3) Krafft, M.P. Controlling phospholipid self-assembly and film properties using highly fluorinated components - Fluorinated monolayers, vesicles, emulsions and microbubbles. *Biochimie* **2012**, *94*, 11–25.

(4) Tang, Y.G.; Yan, J.W.; Zhu, F.; Sun, C.F.; Mao, B.W. Comparative Electrochemical Scanning Tunneling Microscopy Study of Nonionic Fluorosurfactant Zonyl FSN Self-Assembled Monolayers on Au(111) and Au(100): A Potential-Induced Structural Transition. *Langmuir* **2011**, *27*, 943–947.

(5) Oda, R.; Huc, I.; Danino, D.; Talmon, Y. Aggregation Properties and Mixing Behavior of

Hydrocarbon, Fluorocarbon, and Hybrid Hydrocarbon-Fluorocarbon Cationic Dimeric Surfactants. *Langmuir* **2000,** *16*, 9759–9769.

(6) Wang, K.; Karlsson, G.; Almgren, M.; Asakawa, T. Aggregation behavior of cationic fluorosurfactants in water and salt solutions. A cryo-TEM survey. *J. Phys. Chem. B* **1999**, *103*, 9237–46.

(7) Rossi, S.; Karlsson, G.; Ristori, S.; Martini, G.; Edwards, K. Aggregate structures in a dilute aqueous dispersion of a fluorinated-hydrogenated surfactant system. A cryo-transmission electron microscopy study. *Langmuir* **2001**, *17*, 2340–5.

(8) Li, Z.B.; Kesselman, E.; Talmon, Y.; Hillmyer, M.A.; Lodge, T.P. Multicompartment micelles from ABC miktoarm stars in water. *Science* **2004**, *306*, 98–101.

(9) Cui, Z.G.; Fountain, W.; Clark, M.; Jay, M.; Mumper, R.J.; Novel ethanol-in-fluorocarbon microemulsions for topical genetic immunization. *Pharm. Res.* **2003**, *20*, 16–23.

(10) Zu, Y.B.; Gao, Z.Q. Facile and Controllable Loading of Single-Stranded DNA on Gold Nanoparticles. *Anal. Chem.* **2009**, *81*, 8523–8528.

(11) https://kur.web.psi.ch/sans1/SANSSoft/sasfit.html

(12) Alexandridis, P.; Athanassiou, V.; Fukuda, S.; Hatton, T.A. Surface Activity of Poly(ethy1ene oxide)-*block*-Poly(propy1ene oxide)-*block*-Poly(ethy1ene oxide) Copolymers. *Langmuir* **1994**, *10*, 2604–2612.

(13) Eastoe, J.; Paul, A.; Rankin, A.; Wat, R.; Penfold, J.; Webster, J.R.P. Fluorinated nonionic surfactants bearing either CF_3–, or H–CF_2–, terminal groups: adsorption at the surface of aqueous solutions. *Langmuir* **2001**, *17*, 7873–8.

(14) J. S. Pedersen, J.S.; Gerstenberg, M.C. Scattering form factor of block copolymer micelles. *Macromolecules* **1996**, *29*, 1363–1365.

(15) Percus, J.K.; Yevick, G.J. Analysis of classical statistical mechanics by means of collective coordinates. *Phys. Rev.* **1958**, *110*, 1–13.

(16) Schael, F.; Löhmannsröben, H.-G. The deactivation of singlet excited all-trans-1,6 -diphenylhexa-1,3,5-triene by intermolecular charge transfer processes. 1. Mechanisms of fluorescence quenching and of triplet and cation formation. *Chem. Phys.* **1996**, *206*, 193–210.

(16) Esquembre, R.; Ferrer, M.L.; Gutiérrez, M.C.; Mallavia, R.; Mateo, C.R. Fluorescence study of the fluidity and cooperativity of the phase transitions of zwitterionic and anionic

liposomes confined in sol-gel glasses. *J. Phys. Chem. B* **200**7, *111*, 3665–3673.

(17) Mateo, C.R., Lillo, M.P.; Gonzalez-Rodriguez, J.; Acuna, A.U. Molecular Order and Fluidity of the Plasma Membrane of Human Platelets from Time-Resolved Fluorescence Depolarization. *Eur. Biophys. J.* **1991**, *20*, 41–52.

(18) Stähler, K.; Selb, J.; Barthelemy, P.; Pucci, B.; Candau, F. Novel Hydrocarbon and Fluorocarbon Polymerizable Surfactants: Synthesis, Characterization and Mixing Behavior. *Langmuir* **1998**, *14*, 4765–4775

(19) Szajdzinska-Pietek, E.; Wolszczak, M. Time-resolved fluorescence quenching study of aqueous solutions of perfluorinated surfactants with the use of protiated luminophore and quencher. *Langmuir* **2000**, *16*, 1675–1680.